J. Shanghai Jiao Tong Univ. (Sci.), 2019, 24(1): 58-63
https://doi.org/10.1007/s12204-019-2040-3

Dynamic Simulation Analysis of Humanoid Robot Walking System Based on ADAMS

ZHANG Bangcheng[1*] (张邦成), *SHAO Chen*[1] (邵 晨), *LI Yongsheng*[2] (李永生),
TAN Haidong[1] (谭海东), *JIANG Dawei*[3] (姜大伟)
(1. School of Mechatronic Engineering, Changchun University of Technology, Changchun 130012, China;
2. CRCC Changchun Railway Vehicles Co., Ltd., Changchun 130062, China;
3. School of Applied Technology, Changchun University of Technology, Changchun 130012, China)

Abstract: Humanoid robots are a hot topic in the field of robotics research. The walking system is the critical part of the humanoid robot, and the dynamic simulation of the walking system is of great importance. In this paper, the stability of the walking system and the rationality of its structural design are considered in the study of dynamics for a humanoid robot. The dynamic model of humanoid robot walking system is established by using the Lagrange dynamics method. Additionally, the three-dimensional model of CATIA is imported into ADAMS. The humanoid robot walking system is added with the movement of the deputy and the driving force in the ADAMS. The torque and angular velocity of the ankle joint and hip joint are analyzed in the process of knee bends. The simulation results show that the overall performance of the humanoid robot walking system is favorable and has a smooth movement, and the specified actions can be completed, which proves the rationality of the humanoid robot walking system design.
Key words: humanoid robot walking system, Lagrange method, dynamics, ADAMS
CLC number: TP 242 **Document code:** A

0 Introduction

Because the movement performance of the humanoid robot walking system determines the rationality of prototype production and the stability of movement, a simulation analysis is needed to assess whether the design of the walking system meets the requirements. In addition, the design scheme is improved to increase the probability of the successful development of the physical prototype. By combining the dynamics analysis software ADAMS/View module and CATIA, and solving the motion parameters of the main joints, the simulation movement curve is given, and the motion simulation of the walking system is realized. Then, the motion parameters of the humanoid robot are obtained, which provides Ref. for the optimal design of the walking system and the choice of power source.

To study the stability of the humanoid robot walking system, the dynamics of the walking system are studied in this paper. Various theoretical models can be used in the study of dynamic problems. At present, dynamic analysis methods mainly include the Newton Euler method[1], Kane method[2-3] and Lagrange method[4-5]. Reference [6] uses the Newton Euler method to analyse the fully parallel robot. This method is more intuitive, and the concept is clearer. However, considering that the internal force does not work, the amount of calculation is quite large. Reference [7] uses the Kane's method to analyse the bionic robot. The calculation process of this method is recurrent and normative, which is convenient for computer programming. However, because this method needs to calculate the system kinetic energy function, both derivative and integral, it will be difficult to solve. Considering that the humanoid robot walking system is a complex multi-rigid-body system, the Lagrange method can adapt to the motion requirements of fast response and high accuracy, and it also has strong theoretical and logical properties.

In this paper, the Lagrange method is used to simulate the humanoid robot walking system, and dynamic simulation is carried out by ADAMS. The simulation results show that the motion stability of the humanoid robot walking system is verified.

1 Structure Model of Humanoid Robot Walking System

The humanoid robot walking system is the

Received date: 2018-08-13
Foundation item: the Jilin Province Science and Technology Development Project (No. 20150309005YY) and the National Natural Science Foundation of China (No. 51875047)
∗**E-mail:** zhangbangcheng@ccut.edu.cn

anthropopathic design for the robot walking system. The human body can be divided into two large distributions of bones: the bones of the upper limbs and the bones of the lower limbs. Because this paper studies the walking system, only the bones of the lower limbs are described. The bones of the lower limbs can be divided into two major parts: lower limb girdles and bones of the free lower limb. The anthropopathic analysis of the walking system mainly covers the structures of the hip joint, knee joint and ankle joint, as well as research on the method of joint replacement, as shown in Fig. 1.

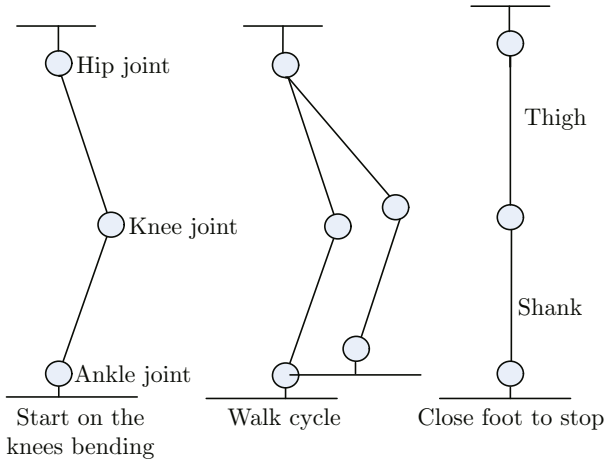

Fig. 1 Kinematic sketch of robot forward motion

It goes without saying that the study of human mimetics is beneficial to the structural design. The motion of the lower limb can be simplified as a rotational motion about an axis that is easier to implement and control in the mechanical structure. From top to bottom, the hip joint can be broken down into three orthogonal axes; the thigh around the X, Y, Z axes can perform a certain range of rotation. The knee joint is mainly used for large angle flexion and extension, and it can be regarded as rotational movement around the axis. The ankle joint can not only can rotate towards the top and bottom of the foot but also rotate inside and outside. To ensure that the completion of the scheduled basic functions is closer to human motion, according to the practicality and cost of design as well as a comfortable range of human lower limb joint movement, the movement range of each joint is designed as shown in Table 1.

2 Simulation Model of Humanoid Robot Walking System

2.1 Format Transformation of Humanoid Robot Walking System Model

ADAMS simulation analysis is mainly used to obtain the dynamic and kinematic parameters of the humanoid robot walking system. If using the ADAMS modelling system, it needs to be modelled again, which will greatly increase the analysis time. To improve design efficiency, the model established in CATIA can be imported into ADAMS. To implement the transfer of the model, as reported in Ref. [8], it relies on SimDesigner$^{\text{TM}}$ (SD) for the CATIA V5 product interface software to be completed. SD can convert the CATIA model to the CMD format, which is the desired model format conversion. To ensure model quality, the assembly and parts are transformed simultaneously. The assembly drawing of the humanoid robot walking system is shown in Fig. 2. After format conversion, the model is imported into the ADAMS/View module as reported in Ref. [9].

Table 1 Lower limb movement range of each joint of the robot

Joint name	Sports name	Movement range
Hip joint	Rotation inward/outward	Outward 45° Inward 45°
	Forward and backward Bend/Extend	Forward 120° Backward 15°
	Adductive/Abductive	Adductive 45° Abductive 45°
Knee joint	Bend/Extend	Forward 90° Backward 0°
Ankle joint (simplified as a two degrees of freedom)	Adductive/Abductive	Left 45° Right 45°
	Bend/Extend	Forward 50° Backward 50°

2.2 Dynamic Modelling of Humanoid Robot Walking System

The results of the dynamic analysis are related to the performance of the whole design. Due to the various models used during computation, there is a large difference in difficulty level and it is very difficult to establish an accurate calculation model with so many moving parts. Each method has some advantages and some

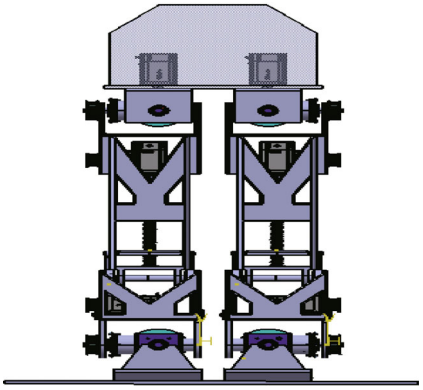

Fig. 2 Assembly drawing of the humanoid robot walking system

disadvantages. By contrast, using the Lagrange dynamic equation to study the dynamics of the humanoid robot walking system is able to ensure the accuracy of the calculation and improve the efficiency of calculation. Therefore, to obtain the dynamic and kinematic parameters of the humanoid robot, the robot walking system model is simplified as a connecting rod motion model. The model can be described as

$$L = K - P, \tag{1}$$

where, K is kinetic energy; P is potential energy; L is the difference of the two values. The dynamic state of the Lagrange equation is described as

$$F_i = \frac{\mathrm{d}}{\mathrm{d}t}\left(\frac{\partial L}{\partial \dot{q}_i} - \frac{\partial L}{\partial q_i}\right), \quad i = 1, 2, \cdots, n, \tag{2}$$

where, i refers to the corresponding connection; F_i, q_i and $\dot{q}_i$ refer to the force of the corresponding connecting rod, rotation angle and velocity, respectively. Suppose a point on the rod motion model is p. The kinetic moment of the connecting rod joint is defined as

$$T_i = \sum_{j=1}^{n} \boldsymbol{D}_{ij}\ddot{q}_i + \boldsymbol{I}_{ai}\ddot{q}_i + \sum_{j=1}^{n}\sum_{k=1}^{n} \boldsymbol{D}_{ijk}\dot{q}_j\dot{q}_k + \boldsymbol{D}_i, \tag{3}$$

where

$$\boldsymbol{D}_{ij} = \sum_{i=\max\{i,j\}}^{n} \mathrm{Trace}\left(\frac{\partial \boldsymbol{T}_p}{\partial q_i}\boldsymbol{I}_p\frac{\partial \boldsymbol{T}_p^{\mathrm{T}}}{\partial q_i}\right), \tag{4}$$

$$\boldsymbol{D}_{ijk} = \sum_{i=\max\{i,j,k\}}^{n} \mathrm{Trace}\left(\frac{\partial \boldsymbol{T}_p}{\partial q_i \partial q_k}\boldsymbol{I}_p\frac{\partial \boldsymbol{T}_p^{\mathrm{T}}}{\partial q_i}\right), \tag{5}$$

$$\boldsymbol{D}_i = -\sum_{p=i}^{n} m_p \boldsymbol{g}^{\mathrm{T}}\frac{\partial \boldsymbol{T}_p}{\partial q_i}{}^{p}\boldsymbol{r}_p, \tag{6}$$

where, $\boldsymbol{I}_{ai}$ refers to the equivalent rotating inertia; ${}^{p}\boldsymbol{r}_p$ refers to the local (relative to point p) position vector in the coordinate system; $\boldsymbol{g}$ refers to the gravitational acceleration; m_p refers to the mass of point p; $\boldsymbol{I}_p$ refers to the pseudo inertia matrix; $\boldsymbol{T}_p$ refers to the transformation matrix.

At this point, the humanoid robot system dynamic model is expressed by the Lagrange dynamic equation, according to the concrete process in Ref. [10].

2.3 Dynamic Simulation of Walking Process of Humanoid Robot

The addition of the motion pair is performed in the Digital Mock-Up (DMU) module in CATIA and is then imported into ADAMS via SimDesigner[11], adding the necessary constraints that could not be added in the DMU. The necessary simplification of the model is carried out, not only defaulting for some parts such as screws and nuts but also regarding the fixed relation of parts such as assembly parts (equivalent to a part) that are assembled in ADAMS; this approach can reduce the computational complexity and computational error. Importing the CATIA model into ADAMS via SimDesigner and the motion pair are shown in Fig. 3.

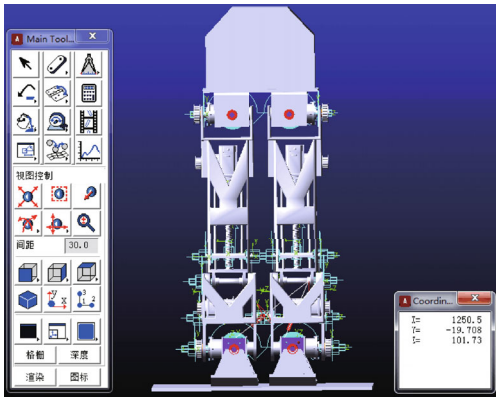

Fig. 3 Schematic diagram of a walking system motion pair

There are three main kinds of motion relations in ADAMS, including lower pairs, higher pairs and basic pairs, which can satisfy most of the motion pair settings. A rotary joint is defined as a rotating pair; there is a relative sliding between the nut and the leg brace, which is defined as the moving pair. These kinematic pairs can be defined and edited directly in ADAMS, and it is necessary to pay attention to the consistency of the defined constraint direction and the actual walking direction; otherwise, it will result in an invalid solution or no solution. For the joint torque setting and constraints, we need to pay attention to the same problem. The knee bend action during walking is the first action to complete, and the ankle and hip joints will withstand higher torque in the process of the first step; thus, the ankle and hip joints are carried on the movement simulation. After adding the motion pair and the drive in the humanoid robot walking system, the virtual prototype model completed by loading is shown in Fig. 4.

The ground option must be set in the simulation; otherwise, it cannot be simulated and analysed and then combined with the actual design of the motion parameters. The analysis time of the ankle joint is set to 25 s, the number of steps is set to 100, and the analysis accuracy error is required to be within 0.001%.

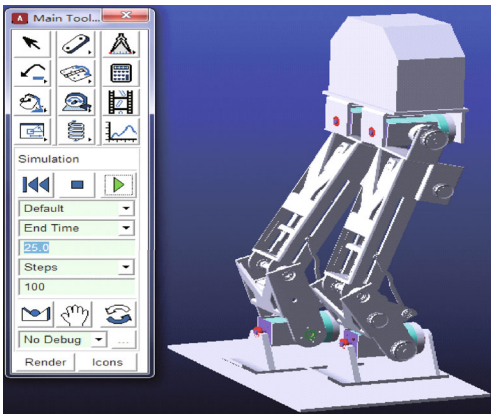

Fig. 4 Virtual prototype simulation analysis of bending knees in the walking system

3 Analysis of Simulation Results

The validity of the constraint and load settings is determined through the analysis of the curve graph and the related animation, which is also reported in Ref. [12]. If correct, the next step is to simulate; if incorrect, we need to modify the parameters. We acquire the velocity change curve and the torque curve, which are obtained by the actual simulation in the motion process. In the following simulation curve, Figs. 5—8 are the torque variation curves of right ankle's lateral and forward rotations in the X, Y, Z directions. Figs. 9—12 are the torque variation curves of the left ankle's lateral and forward rotations in the X, Y, Z directions. Figs. 13—14 are the variation curves of right and left ankle's angular velocity.

As seen from variation curves of the ankle's torque, the maximum torque of right ankle's lateral rotation is in the X direction and is approximately 2.35 N·m

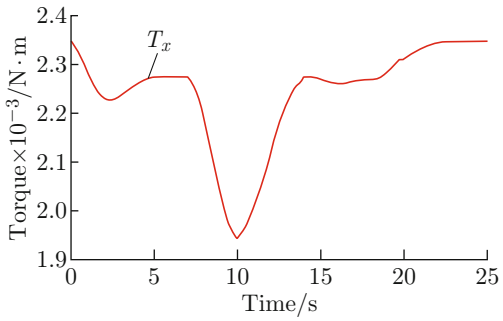

Fig. 5 Torque of the right ankle's lateral rotation in the X direction

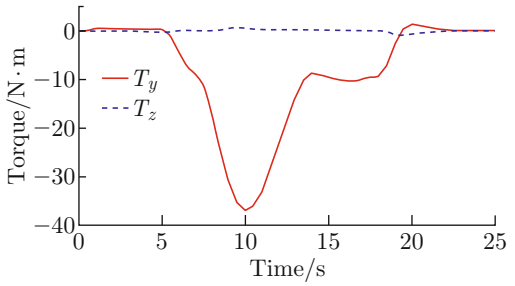

Fig. 6 Torque of the right ankle's lateral rotation in the Y and Z directions

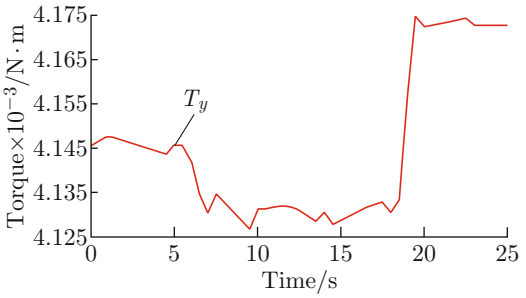

Fig. 7 Torque of the right ankle's forward rotation in the Y direction

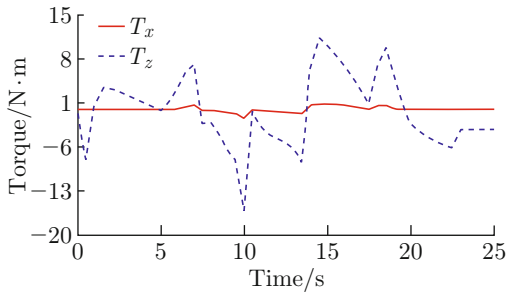

Fig. 8 Torque of the right ankle's forward rotation in the X and Z directions

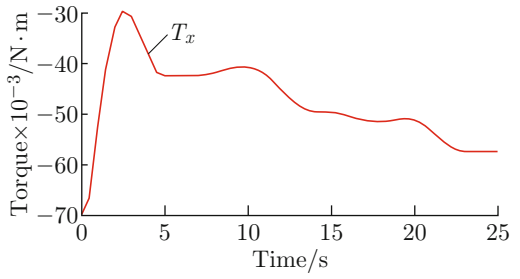

Fig. 9 Torque of the left ankle's lateral rotation in the X direction

(Fig. 5), while the torque in the Y and Z directions is very small (Fig. 6); the maximum torque of the right ankle's forward rotation is in the Y direction, which is approximately 4 175 N·m (Fig. 7), while the torque in the Y and Z directions is very small (Fig. 8); the maximum torque of the left ankle's lateral rotation is in

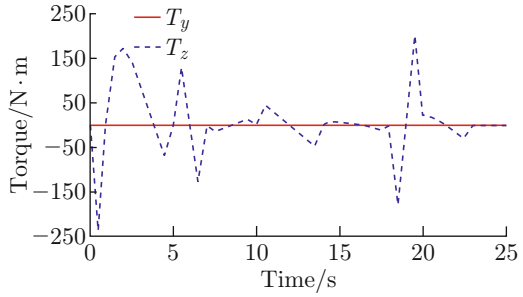

Fig. 10 Torque of the left ankle's lateral rotation in the Y and Z directions

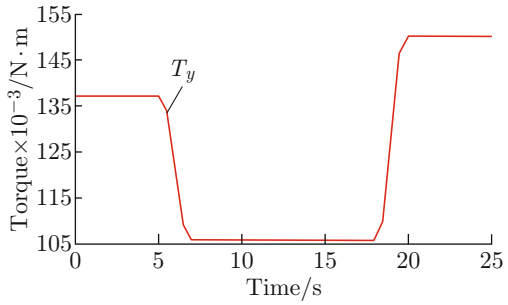

Fig. 11 Torque of the left ankle's forward rotation in the Y direction

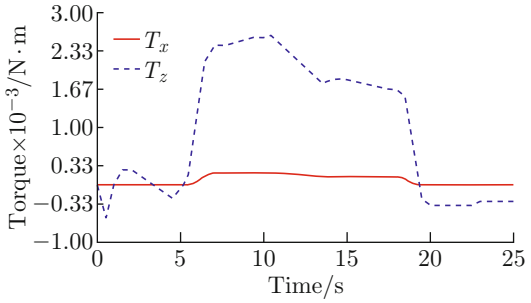

Fig. 12 Torque of the left ankle's forward rotation in the X and Z directions

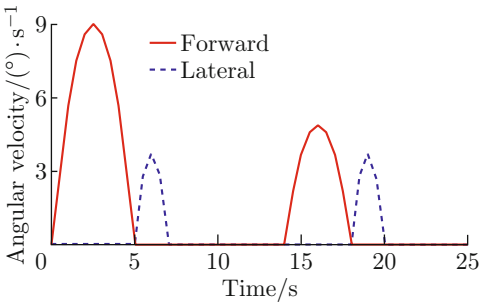

Fig. 13 Variation curves of the right ankle's forward and lateral angular velocity

the X direction, which is approximately $3 \times 10^4\,\mathrm{N \cdot m}$ (Fig. 9), while the torque in the Y and Z directions is very small (Fig. 10); and the maximum torque of the left ankle's forward rotation is in the Y direction (Fig. 11), which is approximately $1.5 \times 10^5\,\mathrm{N \cdot m}$.

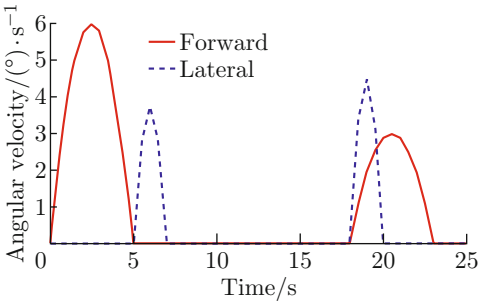

Fig. 14 Variation curves of the left ankle's forward and lateral angular velocity

The analysis results show that the right foot is subjected to bear less torque, as when the right foot is lifted, the left foot is always on the ground. The rotation of the body causes the right ankle joint to withstand a large movement, and the movement occurs in the lateral direction at the front, which is the direction of the rotation of the motor. The movement is consistent with the system's movement.

As seen from the variation curves of each ankle's angular velocity, the rotation directions of the right foot and the left ankle are rather variable in the forward direction. The comparison of Figs. 13 and 14 shows that the left ankle has a front and lateral movement at the same time, while the right foot does not.

The hip is also subjected to increased torque from lifting and dropping the foot. The movement simulation curves of the hip joints are shown in Figs. 15 and 16. The variation curves of angular velocity are shown in Figs. 17 and 18.

As seen from the variation curves of the hip's torque, the maximum torque of the right hip joint occurs in the lateral direction of the right hip. The maximum torque of the left hip joint occurs in the forward direction of rotation, and the left hip is still under the maximum torque, which is similar to the force of the ankle joint. The maximum torque is approximately $135\,\mathrm{N \cdot m}$, and the lateral and forward ankle's variations of the right and left hip joints are relatively independent.

As seen from the variation curves of the angular

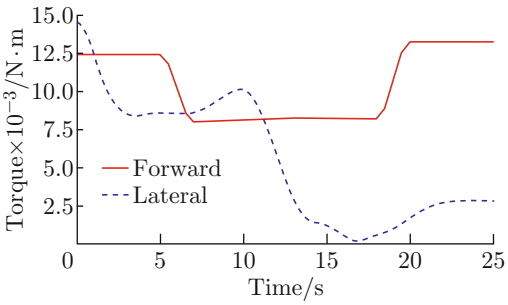

Fig. 15 Variation curves of the right hip's forward and lateral running torque movement of resultant force

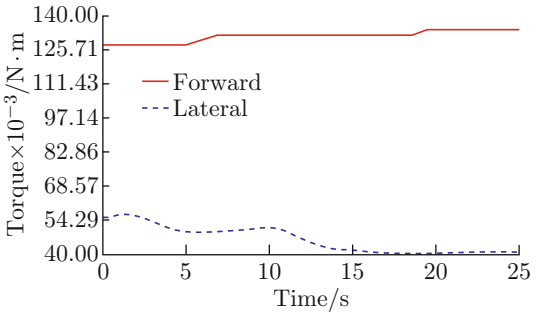

Fig. 16 Variation curves of the left hip's forward and lateral running torque movement of resultant force

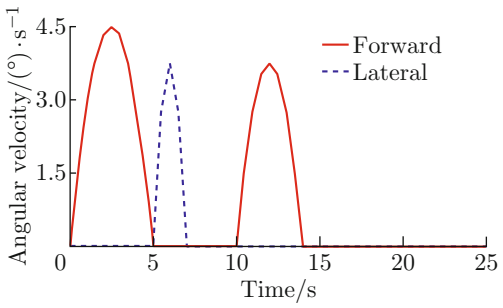

Fig. 17 Variation curves of the right hip's forward and lateral angular velocity

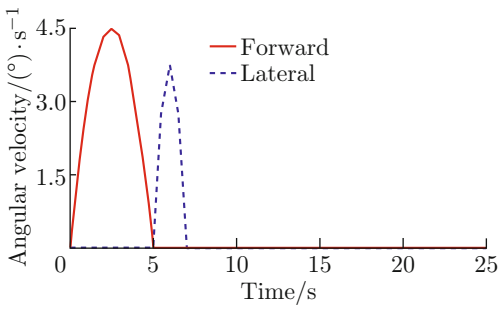

Fig. 18 Variation curves of the left hip's forward and lateral angular velocity

velocity, the ankle joint in the process of accelerating is smooth, and each axis movement of the hip joint changes evenly; such changes can also meet the design requirements of initial stability. According to the above analysis results, unless the force has a certain change, the ankle motion of the humanoid robot is relatively stable. The results verify the rationality of the motor reducer selection and provide reference for the control system design.

4 Conclusion

The stability of the walking system is assessed in the study of dynamics for a humanoid robot in this paper. The Lagrange method is used to simulate the humanoid robot walking system; then, the dynamic simulation is carried out via ADAMS, and the dynamic analysis of the humanoid robot walking system is completed. From the results of the simulation analysis, the torque and angular velocity of the ankle joint and hip joint change uniformly, and there is no violent vibration in the movement of the walking system; thus, the humanoid robot walking system can complete the specified actions smoothly, which proves the rationality of the humanoid robot walking system design.

References

[1] MAEBA T, WANG G, YU F, et al. Motion representation of walking/slipping/turnover for humanoid robot by Newton-Euler method [C]//*SICE Annual Conference*. Tokyo, Japan: IEEE, 2011: 255-260.

[2] GE X F, JIN J T. Dynamics analyze of a dual-arm space robot system based on Kane's method [C]//*2nd International Conference on Industrial Mechatronics and Automation*. Wuhan, China: IEEE, 2010: 646-649.

[3] YANG K, WANG X Y, GE T, et al. A dynamic model of an underwater quadruped walking robot using Kane's method [J]. *Journal of Shanghai Jiao Tong University (Science)*, 2014, **19**(2): 160-168.

[4] LUO L P, YUAN C, SHIN K S, et al. Trajectory for robotic manipulators with torque minimization by using hermit interpolation method [C]//*13th International Conference on Control, Automation and Systems*. Gwangju, Korea: IEEE, 2013: 1480-1483.

[5] CUI M Q. Dynamical modeling of SCARA robot based on Lagrange formulation [J]. *Machinery Design & Manufacture*, 2013(12): 76-78 (in Chinese).

[6] AKBARZADEH A, ENFERADI J, SHARIFNIA M. Dynamics analysis of a 3-RRP spherical parallel manipulator using the natural orthogonal complement [J]. *Multibody System Dynamics*, 2013, **29**(4): 361-380.

[7] WEI H X, WANG T M, LIU M. Inverse dynamic modeling and analysis of a new caterpillar robotic mechanism by Kane's method [J]. *Robotica*, 2013, **31**(3): 493-501.

[8] ZHANG M, WANG P L. Application of MSC SimDesigner in product design [J]. *Computer Aided Engineering*, 2006, **15**(Sup1): 447-449 (in Chinese).

[9] GUO Y. Virtual prototype and dynamics simulation of reducer based on CATIA [D]. Yanbian University, 2012 (in Chinese).

[10] CAI Z X. Robotics [M]. 2nd ed. Beijing: Tsinghua University Press, 2009 (in Chinese).

[11] WANG X P, SHA Y B, ZHAO X Y. Dynamic simulation for clamping manipulator based on ADAMS [J]. *Machine Tool & Hydraulics*, 2013, **41**(13): 142-143(in Chinese).

[12] AN Z L, LI W G, WANG L L, et al. Gait simulation and analysis of humanoid robot based on ADAMS [J]. *Mechanical Engineer*, 2015(4): 57-59 (in Chinese).